Exploring the Physicochemical Properties of Oxime–Reactivation Therapeutics for Cyclosarin, Sarin, Tabun, and VX Inactivated Acetylcholinesterase

4 AUTHORS, INCLUDING:

Emilio Xavier Esposito
exeResearch LLC
27 PUBLICATIONS **337** CITATIONS

Wymore Troy
University of Tennessee
36 PUBLICATIONS **329** CITATIONS

Jeffry D Madura
Duquesne University
160 PUBLICATIONS **19,318** CITATIONS

Exploring the Physicochemical Properties of Oxime-Reactivation Therapeutics for Cyclosarin, Sarin, Tabun, and VX Inactivated Acetylcholinesterase

Emilio Xavier Esposito,*,[†] Terry R. Stouch,[‡] Troy Wymore,[§] and Jeffry D. Madura[⊥,‖]

[†]exeResearch LLC, 32 University Drive, East Lansing, Michigan 48823, United States

[‡]Science For Solutions, LLC, 6211 Kaitlyn Court, Princeton Junction, New Jersey 08550, United States

[§]Oak Ridge National Laboratory, P.O. Box 2008, Oak Ridge, Tennessee 37831, United States

[⊥]Center for Computational Sciences, Department of Chemistry & Biochemistry, Duquesne University, 600 Forbes Avenue, 308 Mellon Hall, Pittsburgh, Pennsylvania 15282, United States

[‖]Department of Chemistry & Biochemistry, Duquesne University, 600 Forbes Avenue, 308 Mellon Hall, Pittsburgh, Pennsylvania 15282, United States

S Supporting Information

ABSTRACT: The inactivation of acetylcholinesterase (AChE) by organophosphorus agent (OP) compounds is a serious problem regardless of how the individual was exposed. The reactivation of OP-inactivated AChE is dependent on the OP conjugate, and commonly a specific oxime is better at reactivating a specific OP conjugate than several diverse OP conjugates. The presented research explores the physicochemical properties needed for the reactivation of OP-inactivated AChE. Four different OPs, cyclosarin, sarin, tabun, and VX, were analyzed using the same set of oxime reactivators. A trial descriptor pool of semiempirical, traditional, and molecular interaction field descriptors was used to construct an ensemble of QSAR models for each OP-conjugate pair. Based on the molecular information and the cross-validation ability, individual QSAR models were selected to be part of an OP-conjugate consensus model. The OP-conjugate specific models provide important insight into the physicochemical properties required to reactivate the OP conjugates of interest. The reactivation of AChE inactivated with either cyclosarin or tabun requires the oxime therapeutic to possess an overall polar-positive surface area. Oxime therapeutics for the reactivation of sarin-inactivated AChE are conformationally dependent while oxime reverse therapeutics for VX require a compact region with a highly hydrophilic region and two positively charged pyridine rings.
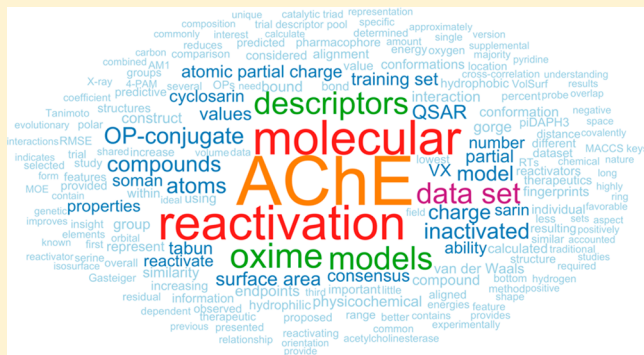
INTRODUCTION

The inactivation of acetylcholinesterase (AChE) by organophosphorus agents (OPs) is not a common occurrence but does happen due to accidental exposures[1] in agricultural settings and or through malicious acts[2,3] to advance political causes. Organophosphorus agents were initially discovered as pesticides by IG Farben in Germany during 1936 and converted to warfare agents during the lead up to World War II.[4] Between World War II and the present day, research has been conducted to develop new OPs as both pesticides and chemical weapons.[4,5] They were pushed into public view as chemical warfare agents during the first Gulf War[6] and again in the spring of 1995 when sarin was used in coordinated attacks on the Tokyo subway.[7,8] The sarin (GB) subway attack in Tokyo is possibly the best-known use of OPs in a terrorist act while the Gulf Wars brought other OPs such as cyclosarin (GF), soman (GD), tabun (GA), and VX, to name a few, forward as wartime weapons. Yet the most frustrating aspect

of OPs is the minimal ability to reactivate OP inactivated AChE. There are several reasons for the difficulty of OP reactivation; one of the most intriguing yet difficult to overcome is the formation of a unique OP conjugate for each OP agent that interacts with the serine at the bottom of the AChE gorge.[9] Thus, sarin has a different OP conjugate compared with VX, tabun, and soman. Another difficulty for the reactivation of OP inactivated AChE is the process of aging.[10−15] After the OP has covalently bound to the serine at the bottom of the gorge and the OP's leaving group has left, there is a period of time before the OP conjugate is hydrolyzed to "age" the OP. The aging results in an OP adduct that is typically more difficult to "remove", aka reactivate, than the initial OP conjugate. A majority of the currently used reactivation therapeutics (RT) for OP inactivated

AChE are positively charged quaternary amines that are not good at passing through the blood—brain barrier to reach inactivated AChE.[16−18] A newly designed, synthesized, and tested collection of amidine-oximes[19−21] are able to cross the blood—brain barrier because of their zwitterionic nature at physiological pH. While the blood—brain barrier obstacle is being overcome, any one of these problems makes it hard to develop and advance a therapeutic but when encountered in combination, as is the case for OP-inactivated AChE, being able to surpass a portion of the above-noted problems is considered a success. The achievement of a broad spectrum RT is a desired but unachieved goal due to the diversity of covalent AChE inactivators.

The AChE gorge is long and narrow (approximately 20 Å long by 7 Å wide) and terminates with a catalytic triad[22] composed of a serine, a glutamic acid and a histidine; Figure 1, part A
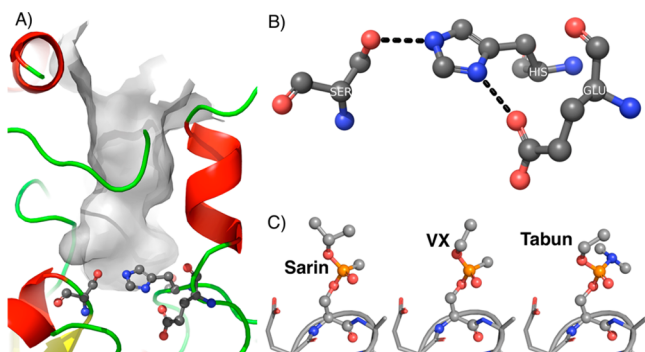
Figure 1. The AChE gorge, catalytic triad, and OP conjugates. (A) The AChE gorge illustrated with the catalytic triad (atoms represented as ball-and-stick) at the bottom of the gorge. (B) The catalytic triad with proton and electron shuttle pathways shown with black dashed lines. (C) The OP conjugates of sarin, VX, and tabun.

(graphical representation of murine AChE, 1j06[23,24] with the molecular surface of the gorge defined by HOLLOW[25]) and part B. The serine residue located at the bottom of the gorge, can covalently bond with an OP resulting in an inactivated AChE. The deep and restrictive path to the catalytic triad complicates the reactivation of OP-inactivated AChE. This constrictive route to and from the catalytic site makes it difficult for RTs to access the OP conjugate, reactivate the AChE, and allow the reactivation therapeutic, and the reconstituted OP to exit the gorge while not re-inactivating or inhibiting the AChE. The structures for three of the four OP conjugates (sarin from 2jgg,[15,23] VX from 2jgh,[15,23] and tabun from 3dl4[14,23]) have been solved and are displayed in Figure 1C. The OP conjugates dictate how and the extent to which the oxime RTs are able to reactivate the inactivated AChE.[26] While these are important aspects to keep in mind regarding the reactivation of inactivated AChE, little attention has been given to the important physicochemical properties of the RT compounds as they relate to the different OP conjugates.

Previous reactivation quantitative structure−activity relationship (QSAR) studies have focused on a single OP conjugate or QSAR methodology or did not explore the physicochemical implications of the proposed models. These previous reactivation QSAR models were constructed from limited trial descriptor pools and thus had restrained applicability to the understanding of important molecular features and did not allow for the essential comparison between QSAR models for different OP-conjugate pairs. This resulted in models that do not always add to the understanding of the molecular properties important for

reactivation or predicting a large number of potential RTs for various OP conjugates.
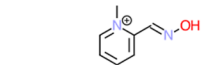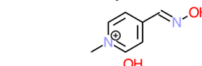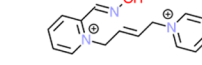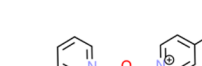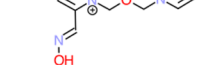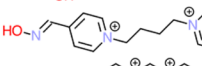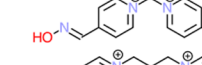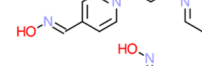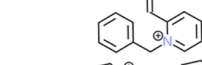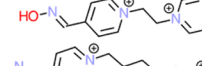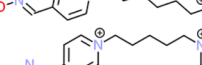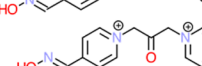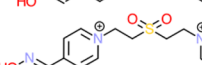
Mager and Seese[27] and Su et al.[28] presented QSAR studies for various sets of oximes capable of reactivating OP-inactivated AChE in the early 1980s. Both groups employed the Hammett−Taft equations[29] to represent the physicochemical property changes of molecules based on electronic structure effects of different substituents. Hansch and Leo[30] provide an extensive discussion of Hammett−Taft QSAR modeling. The models of Mager and Seese and Su et al. are extremely interesting but provide limited molecular insight into the interaction between the oxime RT and the reactivation of inactivated AChE or the similarities and differences for the reactivation of OPs. The oxime RT QSAR models of Mager and Seese[27] demonstrated the important function of lipophilic, specifically the log of the octanol/water partition coefficient, and steric substitution parameters as molecular descriptors for diisopropylfluorophosphate (DFP)-inactivated AChE. Su and co-workers[28] constructed similar types of models for pinacolyl methylphosphonofluoridate (commonly referred to as soman)- and paraoxon-inactivated AChE. The Su et al. models show the importance of the position of the oxime functional group on the pyridinium ring, the Hammett's σ constant (electronic factors), and the log of the octanol/water partition coefficient. Additionally, Su et al. indicate that the reactivation mechanism for PMF by oximes is different than that of paraoxon.

The artificial neural network[31] (ANN) based QSAR model of Dohnal and co-workers[32] uses a unique data set with 17 oxime reactivators for four OP conjugates (cyclosarin, sarin, tabun, and VX) that have inactivated rat AChE. The oximes of the training set were fragmented into nine substructures that represented conserved structural motifs and were used as molecular descriptors. These molecular fragments and the observed reactivation percentages were used to construct the ANN-QSAR model. By using molecular fragments instead of traditional molecular descriptors, the resulting model provided the optimal molecular fragments for each location along the aldoxime scaffold that are important to reactivating the four OP conjugates.
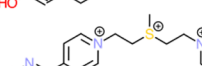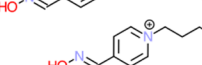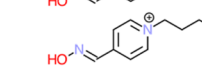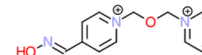
Mager and Weber[33] constructed ANN-QSAR models for a set of aldoximes (similar scaffold structure of HI-6; see Table 1) with reactivation values for soman (15 oximes), paraoxon (15 oximes), and sarin (14 oximes) but only five oximes had end points for the three OP conjugates. It can be considered for this set of oximes, aldoximes, that there is a reactivation group (interacts with the OP conjugate) and an auxiliary group. For all three OP conjugates, it was found that the absolute lowest unoccupied molecular orbital (LUMO) energy was linearly related to the reactivation ability of the oxime. Two other physicochemical properties have inverse parabolic relationships with respect to the reactivation abilities of the oximes. Based on molar refractivity representing steric bulk, a compact or bulky substituent at the auxiliary group location increases reactivation. Improved reactivation is also gained by reactivation therapeutics that are less hydrophilic or very hydrophilic.

The work by Bhattacharjee et al.[34] used a set of 11 oximes with experimental binding affinities to tabun-inactivated mouse AChE. The authors constructed a pharmacophore model also capable of calculating end points. Their quantitative pharmacophore model was applied to four test set compounds (three of the compounds had observed end points) with marginal success. Like the binding affinity aspect of this model, the pharmacophore

Table 1. Oxime Compounds and Associated Percent Reactivation for OP Conjugate Inactivated Rat AChE[a]

		Cyclosarin	Sarin	Tabun	VX
2-PAM		3	36	1	44
4-PAM		3	16	6	35
BI-6		57	32	3	46
HI-6		58	40	2	59
K-074		0	54	46	72
methoxime (MMC-4)		32	21	0	45
trimedoxime (TMB-4)		0	76	41	85
TO-020		0	4	6	6
TO-029		0	44	0	70
TO-033		0	22	2	20
TO-047		0	34	8	41
TO-052		3	44	8	71
TO-057		8	30	8	26
TO-058		0	25	9	46
TO-063		0	16	2	26
TO-092		0	44	8	77
obidoxime		0	41	0	79

[a]Note: The 3D structures with atomic partial charges are provided as a stacked MOL2 file in the Supporting Information.

model provides little insight into the required physical properties for reactivation.

Previous QSAR modeling studies point to an overreaching concern: the OP conjugate covalently bound to the serine of the AChE catalytic site dictates the molecular features needed by the RT to reactive the AChE. The QSAR study presented herein explores, evaluates, and expands the information provided by a set of previously studied oximes reactivators.[32] The creation and analysis of QSAR models, constructed from a trial pool of mixed-class molecular descriptors,[35] is a unique aspect of this study. This is especially true when the protocol is applied to the biological end points (reactivation percentage) for the oxime reactivation of four OP conjugates. The information gained from mixed-class QSAR models[35] provides insight into the important and varied physicochemical properties of RTs for each of the OP conjugates while aiding the overall understanding of a multi-dimensional problem caused by the OP−AChE pairings.

■ METHODS AND PROTOCOLS

The data set, protocols, and methodologies used in this study are presented below. The progression from aligning the training set compounds to calculating the molecular descriptors to constructing the predictive models and the resultant consensus models are presented.

The Oxime Training Set. The training set was collected from a previous QSAR study by Dohnal et al.,[32] discussed above, and contains 17 known AChE reactivators for several OP conjugates (cyclosarin, sarin, tabun, and VX) with reported end points ranging from 0% to 85% reactivation of rat AChE. The biological end points were determined using the Ellman's method,[36] and the ability of the reactivation therapeutic is expressed on a scale of 0% to 100%. Ellman and coworkers[36] developed this colorimetric assay to determine the activity of AChE; an increase of the yellow chromophore produced by thiocholine when reacting with the dithiobisnitrobenzoate ion is measured spectrophotometrically at 405 nm, and thus the solution's colorimetric change indicates an increase in AChE activity. Table 1 contains the oxime RTs and their percent reactivation for cyclosarin, sarin, tabun, and VX.

Molecular Alignment. The alignment of four mouse AChE−oxime complexes (2gyv,[37] 2gyw,[37] 2whr,[38] and 2jez[39]), obtained from the PDB,[23] to each other resulted in the alignment of the bound

conformations of HLö-7, Ortho-7, K-027, and obidoxime, respectively. These mouse AChE structures were selected for the molecular alignments for several reasons but mostly because there are no publicly available rat AChE structures, *apo* or OP-inactivated, with bound oximes to use for the molecular alignment. Because rat AChE end points were used in the creation of the QSAR model, known oxime-based reactivators complexed to mouse AChE were used for the oxime alignment. At the time of this research, only one human AChE complexed with an oxime was publicly available. There are no amino acid or structural differences in the binding site between human and mouse AChE, and thus we expect that there would be no structural differences between human and rat. The structures of OP-inactivated mouse AChE complexed with an oxime are also high-quality structures, resolutions less than or equal to 2.60 Å, R_{values} less than or equal to 0.198, and R_{free} values less than or equal to 0.241; thus this quartet of oximes complexed to mouse AChE was deemed suitable for the oxime alignment. These structures were also used as the alignment template since they were in agreement regarding the location of the oxime group that interacts with the OP conjugate at the bottom of the gorge. Each of the 17 training set compounds were individually aligned to the aligned oximes obtained from the X-ray structures; the X-ray structures were restrained while the training set oximes were allowed to flexibly align to the X-ray structures. A final alignment was performed to refine the molecular alignment between the X-ray structures and the training set compounds. The molecular alignment was performed using the FlexAlign application within MOE 2010.10.[33] Following alignment, the AM1-bond charge correction (AM1-BCC) atomic partial charges[40] were calculated for the training set's proposed bound conformations.

Molecular Similarity. Calculating the amount of molecular similarity, and conversely the dissimilarity, between two compounds is a common tool used for the search of new compounds or, as it was used in this study, a method of determining the diversity of the compounds within a data set. Molecular similarity starts by representing each compound as a series of numbers based on molecular features; this is the molecule's fingerprint.

The MACCS keys[41] molecular fingerprinting and similarity method contains 166 "public" substructural features that include the number of nitrogen−oxygen single bonds (key 24), the number of amine (NH_2) groups (key 84), number of chlorine atoms (key 103), the number of methyl groups four bonds from a methylene group (CH_2) (key 108), the number of methyl groups (key 160), and the number of atoms in rings (key 165). The piDAPH3[33,42,43] molecular fingerprinting method takes into account the compound's 3D structure and the pharmacophore elements (hydrogen bond acceptors, hydrogen bond donors, polar atoms, hydrophobic atoms, anionic atoms, and cationic atoms) associated with individual atoms or groups of atoms. The distance between these pharmacophore elements is measured and then used to construct triangles; the triangles are used to compare the compounds. The piDAPH3 method has eight atom classifications that include hydrogen bond donor (D), hydrogen bond acceptor (A), polar (P; both a hydrogen bond donor and acceptor), and hydrophobic (H). Atoms that are classified as one of these four pharmacophore elements are further defined as those with π-groups. From the collection of pharmacophore elements, all possible triangles are constructed to form the fingerprint.

Once the fingerprints are constructed, the similarity between two compounds is determining by determining the number of shared fingerprint components. Based on the number of fingerprint components in each compound and the number of shared "bits", it is common to calculate the Tanimoto coefficient,[44] although there are other methods to calculate shared molecular similarity,[45] to represent the amount of shared molecular similarity. The Tanimoto coefficient is calculated using the equation

$$\text{Tanimoto coefficient} = \frac{ab}{(a + b - ab)}$$

where a is the number of bits in the fingerprint of compound A, b is the number of bits in that of compound B, and ab is the number of bits shared between compounds A and B. The resulting similarity value is

between 0 and 1 with 0 being no similarity and 1 being a perfect match. Tanimoto coefficients calculated with different fingerprinting methods *cannot* be compared. Thus, a pair of compounds considered molecularly similar to MACCS keys might not be regarded as similar to piDAPH3. The MACCS keys and piDAPH3 molecular fingerprints and the resulting Tanimoto coefficients were calculated in MOE 2010.10.[33]

Molecular Descriptors. The aligned molecules were used to calculate the semiempirical (AM1[46]), traditional 2D, $2^1/_2$D,[47,48] and VolSurf-like molecular descriptors[49−51] for this study's trial descriptor pool. The 2D molecular descriptors, occasionally referred to as traditional descriptors, are the numerical properties evaluated from the connection tables representing a molecule and include physical properties, subdivided surface areas,[47,52,53] atom counts, bond counts, Kier and Hall connectivity and κ shape indices,[54,55] adjacency and distance matrix descriptors containing BCUT[56] and GCUT descriptors, pharmacophore feature descriptors, and partial charge descriptors. The partial charge descriptors are based on the assigned atomic partial charges or the partial equalization of orbital electronegativity atomic partial charges by Gasteiger and Marsili,[57] which are commonly referred to as PEOE or Gasteiger atomic partial charges. A $2^1/_2$D molecular descriptor is defined herein as a 3D molecular property represented as an individual (singular) numerical value. In this case, the $2^1/_2$D molecular descriptors include measures of the conformational potential energy and its components, molecular surfaces, volumes and shapes, and conformation dependent charge descriptors. All of the $2^1/_2$D descriptors are dependent on the conformation of the molecule. Descriptors that indicated toxicity, mutagenesis, or violations of the Lipinski rule of five[58] or Oprea drug-likeness[59] or that required the receptor to calculate an interaction between the oxime and AChE were removed from the trial pool. A description of MOE molecular descriptors is available on the Chemical Computing Group, Inc. website.[60]

The VolSurf molecular descriptors[49−51] are alignment independent, are not strongly dependent on molecular conformation, and like the $2^1/_2$D molecular descriptors represent 3D molecular properties as a single numerical value. The compound is placed in a grid (with the exception of four VolSurf descriptors), a hydrophobic (dry) and hydrophilic (wet) probe visits each grid point, and the interaction energy between the probe and the compound is calculated. The grid points within an interaction energy range are considered an isocontour (isosurface), and the volume is calculated. The calculated volumes and combinations of interaction energies and volumes are used as molecular descriptors. The four nongrid VolSurf descriptors measure the molecular volume, surface area, globularity, and rugosity.

The trial descriptor pool contained 290 molecular descriptors (AM1, 7; 2D and $2^1/_2$D molecular descriptors, 207; VolSurf, 76) calculated within the Molecular Operating Environment (MOE) 2010.10[33] using the MMFF94x molecular force field[33] and Born solvation.[61]

Descriptor Selection and Model Evaluation. Ensembles of QSAR models were constructed using a genetic algorithm[62,63] (also known as a GA) and the previously described trial descriptor pool. A genetic function approximation,[64] a version of a genetic algorithm, was used in this study for molecular descriptor selection with an initial population of 200 models. For each evolutionary step, the top 100 models were subjected to a combination of mutagenesis (60% of the models are mutated) and crossover functions. The top models were (i) mutated, (ii) crossed-over, and (iii) crossed-over and mutated resulting in approximately 250 "new" models, after removing duplicate models, for each evolutionary cycle. The evolution of the training set was considered complete (stable) after 1000 generations with no change in the top 100 models. Each oxime−OP-inactivated AChE data set had five sets of models constructed: models with explicitly two, three, four, or five molecular descriptors and a set of models that allowed the evolutionary process to dictate the number of molecular descriptors (between two and six molecular descriptors). The linear models were evaluated and ranked based on their Q^2 values[65] (leave-one-out cross-validation) throughout and at the end of the evolutionary process. The models were constructed and analyzed using the Opdagelse Predictive Modeling Toolkit[66] (version 1.0) in R[67] (version 2.15.1).

Consensus Models. Models for each end point's consensus model were selected based on their Q^2 values, lack of cross-correlation between

models' residual values, and diversity of the models' molecular descriptor composition. While three to four molecular descriptors are favored based on the traditional "five-to-seven compounds for each molecular descriptor in the QSAR model" rule-of-thumb, models with five or six molecular descriptors were considered for inclusion in the consensus model if they had strong Q^2 values and diverse chemical space. The consensus predicted values for each oxime in the data set are the mean predicted values for the selected QSAR models.

■ RESULTS AND DISCUSSIONS

The reported models contain two to five molecular descriptors and are predictive and informative. A consensus model for each OP conjugate is constructed from an ensemble of models to provide a mean predicted value. Examining the descriptor composition of the individual models provides insight into the unique physicochemical properties responsible for reactivating the various OP conjugates.

Oxime Alignment. The long and flexible nature possessed by most of the oximes can result in unlikely proposed bound conformations for compounds that are built and then energy minimized without any regard to the AChE gorge. The alignment of the training set oximes to the conformations of experimentally determined and AChE bound oximes, regardless whether an OP is covalently bound to the catalytic serine, provides a plausible bound conformation. Molecular descriptor values calculated for the folded conformations would not be representative of the oxime within the AChE's gorge. The proposed bound conformations are depicted in Figure 2 with the four X-ray
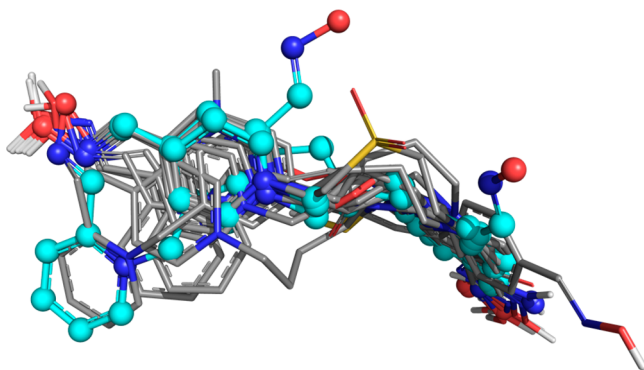
Figure 2. Training set compounds aligned to experimentally determined AChE bound oximes. The four template structures are depicted in cyan ball-and-stick representation, while the training set compounds are gray sticks.

structures used as the template represented as cyan ball-and-sticks and the training set compounds as gray sticks; in both representations oxygen atoms are red and nitrogen atoms are blue. There is agreement between the aligned structures with respect to the location of the oxime group that is proposed to interact with the OP conjugate at the bottom of the gorge. The aligned training set is provided in the Supporting Information section as a stacked MOL2 file with the 3D coordinates and the calculated AM1-BCC atomic partial charges.

The bioactive conformation of oximes proposed by aligning them to experimentally determined conformations of related oximes is important for the calculation of molecular descriptors that are based on the provided 3D molecular structure. Several research groups[33,34] have reported unlikely bound oxime conformations for their ligand-based studies. Specifically, the illustrated oxime RTs of these groups[33,34] are folded in a manner

that prevents the RT from entering the gorge and reaching the OP conjugate.

Training Set Molecular Similarity. Visual inspection of the 17 training set oximes gives the impression that they share much molecular similarity based on fragment and moiety composition. This assumption is reasserted by pairwise molecular similarity using the 166 public MACCS keys,[41] Figure 3B. It could be expected that a RT that works well for VX would be equally able to reactivate cyclosarin, but the similar moiety composition does not translate into the compounds working equally well for the reactivation of different OP conjugates. With the proposed bound conformations of the training set compounds, the piDAPH3 molecular fingerprints[33,42,43] were used for pairwise molecular similarity. Comparing the 3D arrangement of the compound's pharmacophore elements provides some insight into the overall molecular similarity within the training set, Figure 3C. Overall, the training set is rather diverse even though seven compounds have at least one compound that is equivalent, based on piDAPH3 fingerprints, within the training set. It is expected that 2-PAM and 4-PAM are considered identical because they are isomers and small compounds that have limited conformational space. Each RT contains three piDAPH3 pharmacophores: a π-hydrophobe located at the center of the pyridine ring, a π-hydrogen bond acceptor located at the nitrogen of the oxime, and a π-polar at the oxygen of the hydroxyl group of the oxime. These three pharmacophores are in the same 3D location for 2-PAM and 4-PAM, and when the symmetrical compounds methoxime and TO-092 are considered, similar conformations for the pyridine-oxime groups are adopted. Trimedoxime is an augmented version of TO-092, and both contain the same pyridine-oxime moiety as 4-PAM; trimedoxime contains an oxime group at the *para* position of the pyridine. These compounds differ from 2-PAM, 4-PAM, methoxime, and TO-092 by a three carbon aliphatic chain linking the pyridine/pyridine-oxime groups where the middle carbon (CH_2) is classified as a hydrophobe.

QSAR Models. Consensus models were favored over a single QSAR model because they contain multiple overlapping sets of molecular information and are thus able to represent and contain more chemical space while reducing the likelihood of overfitting. The predicted consensus end point for each compound is the mean predicted value of several individual QSAR models. Often, the resulting consensus model has comparable or better R^2, Q^2, and RMSE values than the best individual models. The individual models for each of the OP conjugate consensus models and their associated R^2, Q^2, and RMSE are in Table 2, while the predicted values for each model are provided in the Supporting Information, Tables 1–4.

Cyclosarin Models. The observed end points for this data set range from 0% to 58% reactivation with a majority of the end points at the low extreme (approximately 0% reactivation) resulting in a binary-like data set (active or inactive). Predictive models with two to five descriptors possess Q^2 values between 0.88 and 0.98. The high Q^2 values are a result of the active–inactive nature of the end points, and the resulting models illustrate the key molecular features required for this set of oximes to reactivate cyclosarin-inactivated AChE. Six predictive models were selected to construct the cyclosarin reactivation consensus model.

These six models were combined to form a consensus model with R^2 and Q^2 values of 0.99 and 0.98, respectively, and a RMSE of 2.06% reactivation, see Figure 4. Based on the cross-correlation of residual values among the six models, there is
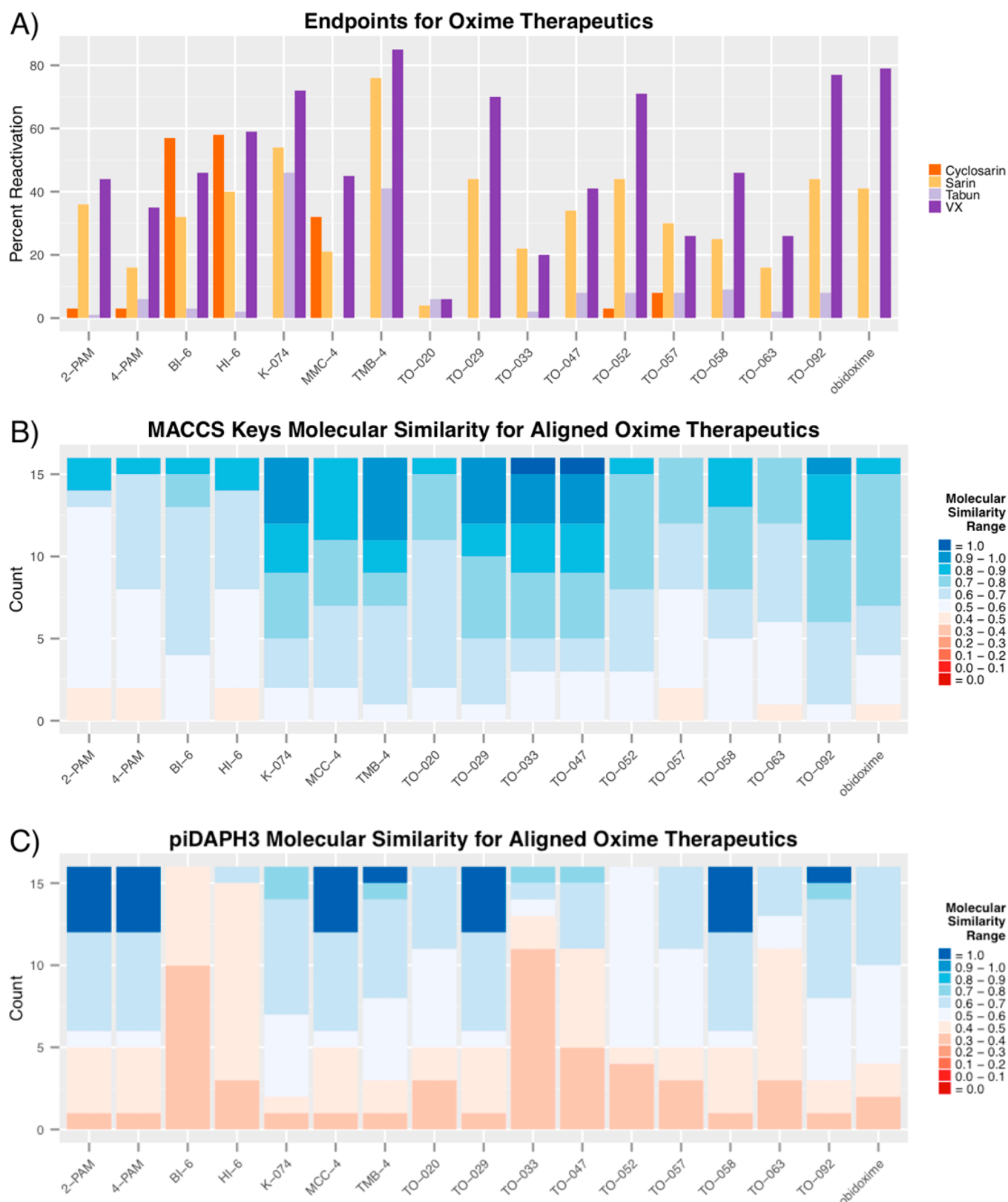
Figure 3. End points and training set molecular similarity. (A) The reactivation values for the oxime therapeutics. The amount of molecular similarity within the training set based on (B) the 166 Public MACCS keys and (C) piDAPH3 molecular fingerprints.

little overlap between the physicochemical properties accounted for in each of the models. The R^2 value between the residuals of any two models ranges from 0 to 0.63. The predicted percent reactivation of methoxime (observed reactivation of 32% and a predicted reactivation ability of 27%) highlights the ability of the consensus model to reliably predict the percentage of cyclosarin−AChE reactivation even though the biological end points are binary-like. An overtrained model would have simply

104

dx.doi.org/10.1021/tx400350b | *Chem. Res. Toxicol.* 2014, 27, 99−110

Table 2. QSAR Models for the Reactivation of Specific OP Inactivated AChE[a]

	R^2	Q^2	RMSE
Cyclosarin			
3.5 + −2.7*radius + 15.2*vsurf_Wp6	0.89	0.88	6.31
−2538.3 + −1745.5*GCUT_SLOGP_0 + 203.7*Q_RPCplus + −44.3*vsurf_CW4 + 2.5*vsurf_Wp4	0.99	0.97	2.16
−2028.1 + −1420.5*GCUT_SLOGP_0 + −14.2*lip_acc + 0.9*vsa_pol + 17.1*vsurf_Wp6	0.98	0.97	2.89
−2568.6 + −1768.5*GCUT_SLOGP_0 + 182.4*Q_RPCplus + −37.6*vsurf_CW4 + 5.7*vsurf_Wp5	0.98	0.96	2.53
−30.3 + −15.2*a_hyd + −70.1*a_nO + −105.2*Q_PCneg + 0.3*VSA + 15.3*vsurf_ID1	0.99	0.98	1.85
−966.7 + 6.0*dipole + −1303.1*GCUT_SMR_0 + 200.2*PEOE_RPCplus + −42.8*vsurf_EWmin3	0.99	0.98	2.24
Sarin			
−232.6 + 138.2*BCUT_PEOE_3 + −30.7*Kier3 + 0.02*pmiX	0.77	0.68	7.89
−92.7 + 90.8*BCUT_SLOGP_3 + −10.9*dipoleY + −40.5*Kier3 + 0.03*pmiX	0.86	0.77	6.12
−194.8 + 11.1*AM1_HOMO + 201.6*BCUT_PEOE_3 + −48.5*Kier3 + 0.03*pmi2	0.85	0.75	6.30
−551.1 + 164.3*balabanJ + 16.7*chi1v + 8.8*E_vdw + −0.1*pmiZ + −0.1*weinerPath	0.92	0.85	4.63
−310.4 + 151.5*BCUT_PEOE_3 + −7.2*chi1v + 4.5*E_vdw + −0.09*pmiZ + −22.6*radius	0.88	0.79	5.73
53.5 + 253.3*BCUT_PEOE_3 + 195.8*BCUT_SLOGP_0 + −38.2*Kier3 + −57.2*npr2 + 0.03*pmiX	0.91	0.86	4.80
Tabun			
880.2 + 1595.7*GCUT_SMR_0 + 0.23*PEOE_VSAplus3 + 4.8*vsurf_DD13	0.81	0.65	5.76
1083.9 + 2.1*E_ang + 1955.0*GCUT_SMR_0 + −0.7*PEOE_VSAneg0 + 5.3*vsurf_DD13	0.97	0.90	2.41
950.6 + 1.3*E_strain + 1706.1*GCUT_SMR_0 + −0.4*PEOE_VSAneg0 + 4.7*vsurf_DD13	0.94	0.85	3.28
1146.7 + 2.0*E_ang + −37.0*FASAneg + 2045.3*GCUT_SMR_0 + −0.7*PEOE_VSAneg0 + 5.3*vsurf_DD13	0.98	0.94	1.95
VX			
11.0 + 36.5*FCharge + −0.1*pmiZ + −3.5*vsurf_DW13	0.88	0.84	7.78
−189.4 + −19.5*AM1_HOMO + −64.2*FASA_H + −1.2*SlogP_VSA4 + −4.0*vsurf_DW13	0.90	0.88	7.07
1157.4 + 2374.5*GCUT_SMR_0 + 11.1*opr_brigid + −16.8*PEOE_PCplus + −0.2*pmiZ + −35.8*vsurf_EWmin1	0.98	0.95	3.28
1168.6 + 9.5*a_aro + 2268.5*GCUT_SMR_0 + −0.02*pmiY + −0.1*pmiZ + −20.2*vsurf_EWmin2	0.97	0.95	3.86

[a]Note: The predicted reactivation of OP-inactivated AChE for each oxime is provided in the Supporting Information.

classified the compound as an activator or not with respect to reactivation of inactivated cyclosarin−AChE.

Analysis of the molecular descriptors indicates that positive atomic partial charges based on semiempirical AM1 calculations (Q_RPCplus; relative positive atomic partial charge) improves the oximes ability to reactivate cyclosarin-inactivated AChE; this molecular feature is mirrored in model 6 where an increase in the negative partial charge, also based on AM1 calculations, reduces the oxime's ability to reactivate cyclosarin. The number of oxygen atoms (a_nO) and the number of oxygen and nitrogen atoms (lip_acc) are tied to a reduction in the reactivation ability of oximes. These descriptors are highly correlated ($R = 0.93$) because one includes the other's molecular feature, oxygen atoms. Increasing the number of hydrophobic atoms (a_hyd) reduces the ability of the oxime to reactivate cyclosarin AChE yet is correlated ($R = 0.89$) to VSA (van der Waals, vdW, surface area), which indicates in the same model that an increase in vdW surface area improves the reactivation ability of these oximes. The molecular descriptors work together indicating that increased surface area is acceptable as long as the increase is not due to hydrophobic (greasy) atoms. Adding to desire for increase surface area that is not hydrophobic is the VolSurf polar isosurface (vsurf_Wp4, vsurf_Wp5 and vsurf_Wp6; volume) molecular descriptor in the range of −2 to −4 kcal/mol, see Figure 5. Increasing the volume of the polar isosurface will improve the reactivation ability of this set of oximes against cyclosarin OP conjugates.

Sarin Models. The observed end points for this data set range from 4% to 76% reactivation of sarin-inactivated AChE. Six predictive models with three to five descriptors and possessing Q^2 values between 0.68 and 0.86 were selected for the sarin reactivation consensus model.

These six models were combined to form a consensus model with R^2 and Q^2 values of 0.91 and 0.86, respectively, and a RMSE

of 4.92% reactivation, see Figure 4. According to the cross-correlation of residual values among the six models, there is little overlap between the physicochemical properties and their influence accounted for in each of the models. The R^2 value between the residuals of any two models ranges from 0.12 to 0.59.

The common and key molecular descriptors for the sarin reactivator QSAR models are not straightforward with respect to being able to indicate prominent chemically based molecular features. The molecular descriptors Kier3 and pmiX are combined in four of the six individual sarin reactivation QSAR models. Kier3 is the third κ shape index and is the comparison of the provided molecule's torsion angles to a linear and fully connected graph representation of the molecule's heavy atoms.[54] The principal moment of inertia molecular descriptors calculated in this study represent the amount of kinetic energy from the center of mass in one of the three Cartesian coordinates, but these descriptors can be used to describe a compound's shape and conformation.[68] The pmiX and pmiZ molecular descriptors are based on the conformation and orientation of the compound; respectively, these descriptors are the X- and Z-component of the principal moment of inertia. The inclusion of molecular descriptors that take into consideration the compound's orientation in three-dimensional space is possible because all the reactivators were aligned based on experimentally determined conformations of known oximes bound in the AChE gorge. The E_vdw and pmiZ molecular descriptors occur as a group in two models indicating that they could represent an overall molecular feature related to the compound's conformation and orientation, the size and shape of the compound.

The E_vdw is the van der Waals term of the oxime's potential energy equation and can be interpreted as an indication of energetic distance from an ideal three-dimensional structure based on atomic clashes. The possibility of a compound having
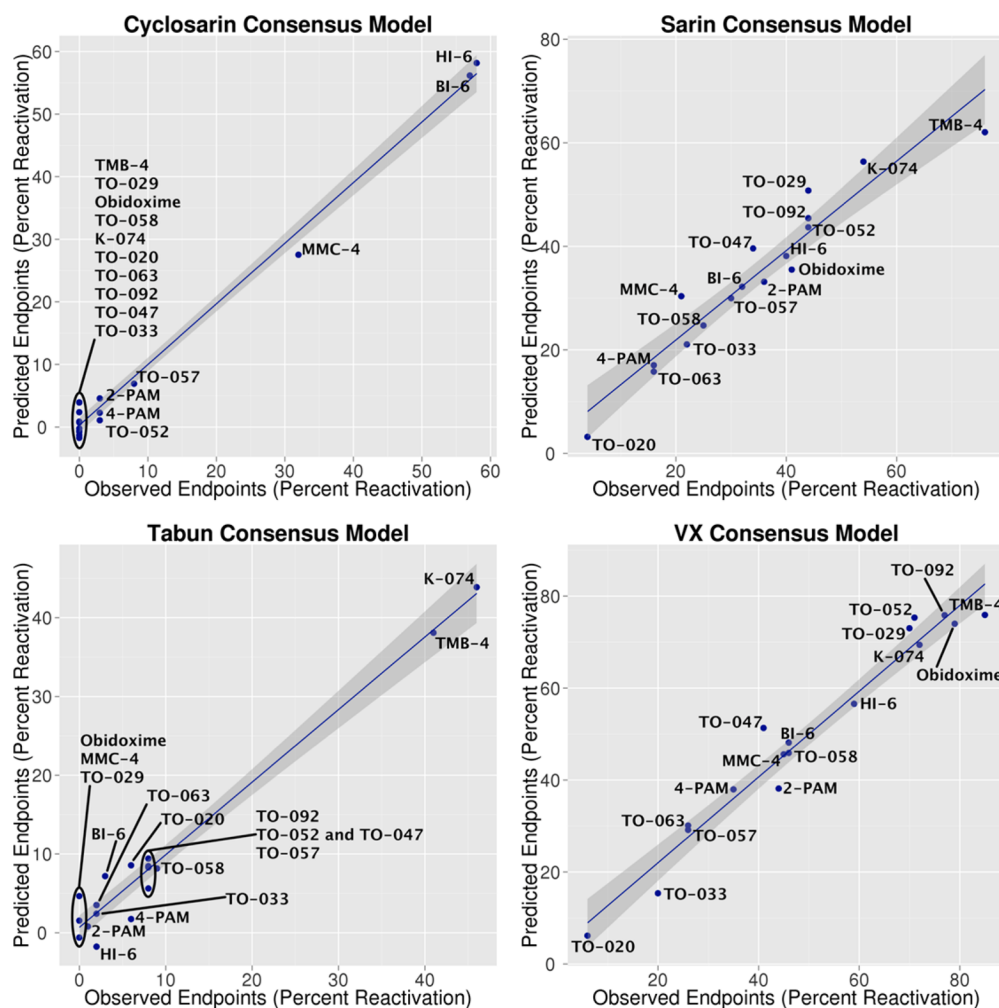
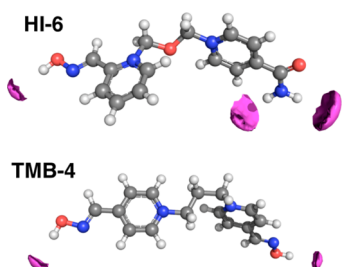**Figure 4.** Observed versus predicted plots.

Figure 5. Polar molecular interaction fields. Comparison of HI-6 (58% reactivation of cyclosarin) to TMB-4 (unable to reactivate cyclosarin inactivated AChE) with the polar probe of the VolSurf molecular interaction field descriptors at −3 kcal/mol, vsurf_Wp5.

steric clashes because it is in a less than ideal conformation is likely because the compounds were aligned to AChE bound oximes.

The BCUT_PEOE_3 molecular descriptor is also present in four of the six models but not the same four models as Kier3 and pmiX and is the mathematical representation of Gastieger atomic partial charges as they relate to the formal bond order within the compound. It is hard to deduce chemically intuitive information from this specific descriptor, and it is used more as a guide; the larger a reactivator's BCUT_PEOE_3 value, the better it is able to reactivate sarin-inactivated AChE. The BCUT molecular descriptors are the mathematical representation of a specified

type of molecular information derived from the structure whether it is atomic partial charges, molar refractivity, or calculated log P (octanol/water partition coefficients). A majority of the molecular descriptors that comprise the QSAR models, with the noted exception of the BCUT and E_vdw descriptors, represent the shape and conformation of compounds. The conformation and orientation of the oxime RT in the AChE gorge is a dominant molecular feature that along with other subtle physicochemical properties aid in the reactivation of sarin-inactivated AChE.

Tabun Models. The observed end points for this data set range from 0% to 46% reactivation with a majority of the end points indicating that this set of compounds is not adept at reactivating tabun-inactivated AChE. The low overall ability of this data set to reactivate tabun-inactivated AChE is reinforced with a majority of the reactivation percentages being less than 10% and the best two reactivators (trimedoxime and K-074) only able to reactivate less than 41% and 46% of the inactivated AChE, respectively. This data set is considered a binary-like data set (active or inactive) with predictive models possessing three to five descriptors and Q^2 values between 0.65 and 0.94. The high Q^2 values are a result of the active−inactive nature of the end points, and the resulting models illustrate the key molecular features required for this set of oxime to reactivate tabun-inactivated AChE. Four predictive models were selected to construct the tabun reactivation consensus model.

These four models were combined to form a consensus model with R^2 and Q^2 values of 0.97 and 0.91, respectively, and a RMSE of 2.48% reactivation, see Figure 4. Based on the cross-correlation of residual values among the four models, there is little overlap between the physicochemical properties accounted for in the models.

The molecular descriptors of interest center on atomic partial charge mapped to the molecular surface and conformation of the molecules. In each model, the vsurf_DD13 descriptor is present; this descriptor is based on the distance between the physical location of the lowest and second-lowest hydrophobic energy interaction between the compound of interest and the probe; see Figure 6. The vsurf_DD13 and vsurf_DD23 (present in a single
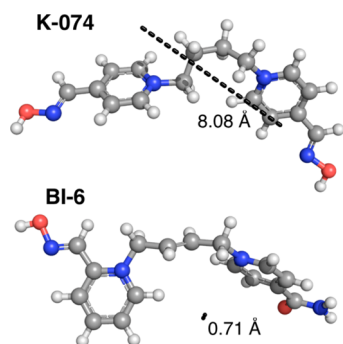
Figure 6. Through-space relationship of the first and third most favorable hydrophobic interactions. Comparison of K-074 (46% reactivation of tabun) to BI-6 (3% reactivation of tabun) for the molecular interaction field vsurf_DD13.

model) descriptors are constructive and by increasing the distance between these three points (the lowest, second-lowest, and third-lowest hydrophobic interaction energies) the compounds are considered better tabun-inactivated AChE reactivators. The PEOE_VSAplus3 (constructive) and PEOE_VSAneg0 (destructive) molecular descriptors are based on the connection table approximate of each atom's van der Waals surface area determined by Gasteiger atomic partial charges. The PEOE_VSAplus3 descriptor indicates that the reactivators of interest increase in their ability to reactivate tabun-inactivated AChE as the surface area of atoms with a Gasteiger atomic partial charge between 0.15 and 0.20 increases. The PEOE_VSAneg0 descriptor signals that increasing the idealized surface area of atoms with Gasteiger atomic partial charge between −0.05 and 0.00 reduces the compounds ability to reactive tabun-inactivated AChE; this is illustrated in Figure 7 for TO-058 (a 9% reactivator of tabun OP conjugates) and obidoxime (unable to reactivate tabun). Continuing the theme of atomic surface area based on atomic charge are the FASAneg and DASA molecular descriptors; these two descriptors are based on the provided three-dimensional conformation of the compound and the AM1 atomic partial charges. FASAneg is the fraction of water (solvent) accessible surface area contributed by atoms with atomic partial charges less than zero, while DASA is the absolute difference between the positive (greater than zero) and negative (less than zero) solvent accessible surface area. The tabun-inactivated AChE reactivation trend is the same for these descriptors as the Gasteiger atomic partial charge−van der Waals surface area descriptors; increasing the surface area associated with positively charged atoms increases the compound's reactivation ability while increasing the negatively charged surface area reduces the compound's reactivation ability.
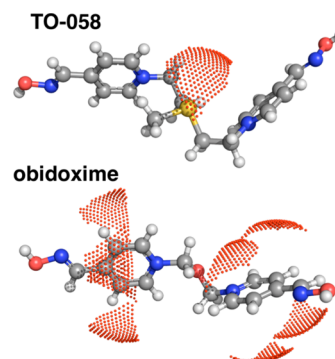

Figure 7. Comparison of van der Waals ideal surface area. The dots represent the van der Waals surface area of atoms with Gasteiger atomic partial charges between −0.05 and 0.00 (PEOE_VSAneg0). The VSA is compared between TO-058 (9% reactivation of tabun) and obidoxime (no ability to reactivate tabun-inactivated AChE).

VX Models. The observed end points for this data set range from 6% to 85% reactivation of VX-inactivated AChE. The consensus model is comprised of four predictive models with three to five descriptors and possessing Q^2 values between 0.84 and 0.95.

The consensus model has R^2 and Q^2 values of 0.96 and 0.94, respectively, and a RMSE of 4.56% reactivation, see Figure 4. According to the cross-correlation of residual values among the four models, there is little overlap between the physicochemical properties accounted for in each of the models; the R^2 value between the residuals of any two models ranges from 0.063 to 0.77.

The lowest hydrophilic (water-loving) interaction energies (vsurf_EWmin1 and vsurf_EWmin2) and the through-space distance between the grid points that correspond to the first and third lowest hydrophilic interaction energies (vsurf_DW13) play a key role in the prediction of the oximes' reactivation of VX-inactivated AChE. Increasing the distance between the first and third lowest hydrophilic interaction energies (vsurf_DW13) reduces the reactivation therapeutic's abilities, see Figure 8 for a
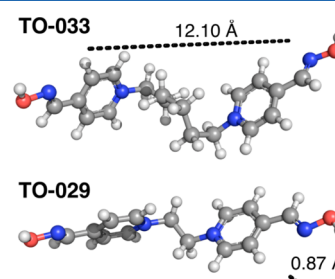
Figure 8. Through-space relationship of the first and third most favorable hydrophilic interactions. Comparison of TO-033 (20% reactivation of VX) to TO-029 (70% reactivation of VX) for the molecular interaction field vsurf_DW13.

comparison between TO-033 (a moderate reactivator, 20%) and TO-029 (a strong reactivator, 70%), while more negative interactions, and thus favorable, between the hydrophilic probe and the compound of interest (represented by the vsurf_EWmin1 and vsurf_EWmin2 descriptors) increases the predicted reactivation ability of the therapeutics. These descriptors are linked and illustrate the need for the lowest hydrophilic interaction energies to be central to a specific location and negative (highly favorable). The number of aromatic atoms and

the number of rigid bonds[59] are highly correlated ($R = 0.99$), and for this data set, reactivation therapeutics with more aromatic atoms or that are more rigid are better able to reactivate VX-inactivated AChE. These descriptors may point to the need for π–π stacking or π–CH_3 interactions between the therapeutic and the active site to correctly position the oxime near the OP conjugate. The π–π stacking is exhibited in several solved cocrystal structures of oximes bound to the gorge of AChE, see PDBs 2gyv,[37] 2gyw,[37] 2whr,[38] and 2jez.[39] Increasing the amount of idealized van der Waals and solvent accessible surface area of atoms with positive atomic charges is detrimental to the reactivation of VX-inactivated AChE. Similarly, increasing the van der Waals surface area of atoms with a SlogP[69] contribution value greater than 0.10 but less than or equal to 0.15 also reduces the ability of the therapeutic. All oximes in this data set have at least one atom with a SlogP contribution within this range, the carbon atom of the six-member ring bonded to the oxime group, with an ideal vdW surface area of approximately 2.7 Å². BI-6 has two additional atoms with SlogP contribution values within this range. The first atom is the oxygen atom of the amide group and the other is the carbon atom of the six-member ring bonded to the amide group.

CONCLUSION

The main aspect of this QSAR study is the insight furnished regarding the important physicochemical properties for this set of oximes to reactivate these four OP conjugates. The two binary data sets, cyclosarin and tabun, do not share reactivating compounds, yet the QSAR models demonstrate the need for increased polar-positive surface area to improve reactivation. Increasing the volume of the polar isosurface while reducing the number of oxygen atoms also improves cyclosarin OP-conjugated AChE reactivation. A defining characteristic of the tabun reactivators is the distance, between 5 and 8 Å, between the most hydrophobic surface locations of the oxime RTs. The sarin reactivators need to adopt a conformation similar to the experimentally determined bound conformations to improve reactivation. The molecular features of VX reactivators are the two positively charged pyridine rings, a compact region of high hydrophilicity and an overall hydrophilic nature that improves reactivation. The models presented herein represent an initial step toward the better understanding of the significant physicochemical properties for the reactivation of OP-inactivated AChE.

ASSOCIATED CONTENT

Ⓢ Supporting Information

The 3D structure of the oxime compounds and their atomic partial charges in a stacked MOL2 file for the training set and the individual model and consensus model predictions for each OP end point along with the consensus predictions, residual values, and standard deviation. This material is available free of charge via the Internet at http://pubs.acs.org.

AUTHOR INFORMATION

Corresponding Author

*Voice: +1.517.639.0684. E-mail: emilio@exeResearch.com.

Notes

The authors declare no competing financial interest.

ABBREVIATIONS

AChE, acetylcholinesterase; AM1, Austin method 1; AM1-BCC, Austin method 1–bond charge correction; ANN, artificial neural network; HOMO, highest occupied molecular orbital; LUMO, lowest unoccupied molecular orbital; OP, organophosphorus agents; PEOE, partial equalization of orbital electronegativity; Q^2, cross-validation coefficient; RMSE, root mean squared error; RT, reverse therapeutic; QSAR, quantitative structure–activity relationship; vdW, van der Waals; VSA, van der Waals surface area

REFERENCES

(1) Than, K. Organophosphates: A Common But Deadly Pesticide, National Geographic, http://news.nationalgeographic.com/news/2013/07/130718-organophosphates-pesticides-indian-food-poisoning/, accessed August 24, 2013.

(2) Gordon, M. R., and Landler, M. Kerry Cites Clear Evidence of Chemical Weapon Use in Syria, In *The New York Times*; The New York Times: New York. http://www.nytimes.com/2013/08/27/world/middleeast/syria-assad.html, accessed August 27, 2013.

(3) Japanese Cult Carries Out Sarin Gas Attack on Tokyo Subway, In *The New York Times*; The New York Times: New York. http://learning.blogs.nytimes.com/2012/03/20/march-20-1995-japanese-cult-carries-out-sarin-gas-attack-on-tokyo-subway/, accessed March 20, 2012.

(4) Tucker, J. B. (2006) *War of Nerves: Chemical Warfare from World War I to al-Qaeda*, Pantheon Books, New York.

(5) Mirzayanov, V. S. (2009) *State Secrets: An insider's chronicle of the Russian chemical weapons program*, Outskirts Press, Inc, Denver, CO.

(6) Petroianu, G. A., Arafat, K., Nurulain, S. M., Kuca, K., and Kassa, J. (2007) In vitro oxime reactivation of red blood cell acetylcholinesterase inhibited by methyl-paraoxon. *J. Appl. Toxicol.* 27, 168–175.

(7) Ogawa, Y., Yamamura, Y., Ando, H., Kadokura, M., Agata, T., Fukumoto, M., Satake, T., Machida, K., Sakai, O., Miyata, Y., Nonaka, H., Nakajima, K., Hamaya, S., Miyazaki, S., Ohida, M., Yoshioka, T., Takagi, S., and Shimizu, H. (1999) An Attack with Sarin Nerve Gas on the Tokyo Subway System and Its Effects on Victims, in *Natural and Selected Synthetic Toxins* (Tu, A. T., and Gaffield, W., Eds.), pp 333–355, American Chemical Society, Washington, D.C.

(8) Tu, A. T. (1999) Overview of Sarin Terrorist Attacks in Japan, in *Natural and Selected Synthetic Toxins* (Tu, A. T., and Gaffield, W., Eds.), pp 304–317, American Chemical Society, Washington, D.C.

(9) Järv, J., Aaviksaar, A., Godovikov, N., and Lobanov, D. (1977) The arrangement of substrate and organophosphorus-inhibitor leaving groups in acetylcholinesterase active site. *Biochem. J.* 167, 823–825.

(10) Millard, C. B., Kryger, G., Ordentlich, A., Greenblatt, H. M., Harel, M., Raves, M. L., Segall, Y., Barak, D., Shafferman, A., Silman, I., and Sussman, J. L. (1999) Crystal structures of aged phosphonylated acetylcholinesterase: Nerve agent reaction products at the atomic level. *Biochemistry* 38, 7032–7039.

(11) Worek, F., Aurbek, N., Koller, M., Becker, C., Eyer, P., and Thiermann, H. (2007) Kinetic analysis of reactivation and aging of human acetylcholinesterase inhibited by different phosphoramidates. *Biochem. Pharmacol.* 73, 1807–1817.

(12) Worek, F., Aurbek, N., Wille, T., Eyer, P., and Thiermann, H. (2011) Kinetic analysis of interactions of paraoxon and oximes with human, Rhesus monkey, swine, rabbit, rat and guinea pig acetylcholinesterase. *Toxicol. Lett.* 200, 19–23.

(13) Carletti, E., Colletier, J.-P., Dupeux, F., Trovaslet, M., Masson, P., and Nachon, F. (2010) Structural Evidence That Human Acetylcholinesterase Inhibited by Tabun Ages through O-Dealkylation. *J. Med. Chem.* 53, 4002–4008.

(14) Carletti, E., Li, H., Li, B., Ekström, F., Nicolet, Y., Loiodice, M., Gillon, E., Froment, M., Lockridge, O., Schopfer, L., Masson, P., and

Nachon, F. (2008) Aging of Cholinesterases Phosphylated by Tabun Proceeds through O-Dealkylation. *J. Am. Chem. Soc. 130*, 16011−16020.

(15) Hörnberg, A., Tunemalm, A.-K., and Ekström, F. (2007) Crystal structures of acetylcholinesterase in complex with organophosphorus compounds suggest that the acyl pocket modulates the aging reaction by precluding the formation of the trigonal bipyramidal transition state. *Biochemistry 46*, 4815−4825.

(16) Karasova, J. Z., Pohanka, M., Musilek, K., Zemek, F., and Kuca, K. (2010) Passive diffusion of acetylcholinesterase oxime reactivators through the blood-brain barrier: Influence of molecular structure. *Toxicol. In Vitro 24*, 1838−1844.

(17) Karasova, J. Z., Stodulka, P., and Kuca, K. (2010) In vitro screening of blood-brain barrier penetration of clinically used acetylcholinesterase reactivators. *J. Appl. Biomed. 8*, 35−40.

(18) Voicu, V. A., Bajgar, J., Medvedovici, A., Radulescu, F. S., and Miron, D. S. (2010) Pharmacokinetics and pharmacodynamics of some oximes and associated therapeutic consequences: A critical review. *J. Appl. Toxicol. 30*, 719−729.

(19) Kalisiak, J., Ralph, E. C., and Cashman, J. R. (2012) Nonquaternary Reactivators for Organophosphate-Inhibited Cholinesterases. *J. Med. Chem. 55*, 465−474.

(20) Kalisiak, J., Ralph, E. C., Zhang, J., and Cashman, J. R. (2011) Amidine-Oximes: Reactivators for Organophosphate Exposure. *J. Med. Chem. 54*, 3319−3330.

(21) Okolotowicz, K. J., Dwyer, M., Smith, E., and Cashman, J. R. (2014) Preclinical Studies of Noncharged Oxime Reactivators for Organophosphate Exposure. *J. Biochem. Mol. Toxicol. 28*, 23−31.

(22) Shafferman, A., Kronman, C., Flashner, Y., Leitner, M., Grosfeld, H., Ordentlich, A., Gozes, Y., Cohen, S., Ariel, N., and Barak, D. (1992) Mutagenesis of human acetylcholinesterase. Identification of residues involved in catalytic activity and in polypeptide folding. *J. Biol. Chem. 267*, 17640−17648.

(23) Berman, H. M., Westbrook, J., Feng, Z., Gilliland, G., Bhat, T. N., Weissig, H., Shindyalov, I. N., and Bourne, P. E. (2000) The Protein Data Bank. *Nucleic Acids Res. 28*, 235−242.

(24) Bourne, Y., Taylor, P., Radic, Z., and Marchot, P. (2003) Structural insights into ligand interactions at the acetylcholinesterase peripheral anionic site. *EMBO J. 22*, 1−12.

(25) Ho, B. K., and Gruswitz, F. (2008) HOLLOW: Generating accurate representations of channel and interior surfaces in molecular structures. *BMC Struct. Biol. 8*, 49.

(26) Antonijevic, B., and Stojiljkovic, M. P. (2007) Unequal efficacy of pyridinium oximes in acute organophosphate poisoning. *Clin. Med. Res. 5*, 71−82.

(27) Mager, P. P., and Seese, A. (1982) Organophosphorus Pesticides and Mammalicides: A Mathematical Study on Chemical Structure and Biological Activity Applied to Parameters for Inhibition of Myoneural Junctions, Axon Demyelination, and Reactivation of Poisoned Acetylcholinesterase. *Zool. Jahrb., Abt. Anat. Ontog. Tiere 107*, 46−70.

(28) Su, C., Tang, C., Ma, C., Shih, Y., and Liu, C. (1983) Quantitative structure-activity relationships and possible mechanisms of action of bispyridinium oximes as antidotes against pinacolyl methylphosphono-fluoridate. *Fundam. Appl. Toxicol. 3*, 271−277.

(29) Hammett, L. P. (1935) Some Relations between Reaction Rates and Equilibrium Constants. *Chem. Rev. 17*, 125−136.

(30) Hansch, C., and Leo, A. (1995) *Exploring QSAR: Fundamentals and applications in chemistry and biology*, American Chemical Society, Washington, DC.

(31) Schneider, G., and Wrede, P. (1998) Artificial Neural Networks for Computer-Based Molecular Design. *Prog. Biophys. Mol. Biol. 70*, 175−222.

(32) Dohnal, V., Kuca, K., and Jun, D. (2005) Prediction of a new broad-spectrum reactivator capable of reactivating acetylcholinesterase inhibited by nerve agents. *J. Appl. Biomed. 3*, 139−145.

(33) Mager, P., and Weber, A. (2003) Structural Bioinformatics and QSAR Analysis Applied to the Acetylcholinesterase and Bispyridinium Aldoximes. *Drug Des. Discovery 18*, 127−150.

(34) Bhattacharjee, A. K., Kuca, K., Musilek, K., and Gordon, R. K. (2010) In silico pharmacophore model for tabun-inhibited acetylcho-

linesterase reactivators: A study of their stereoelectronic properties. *Chem. Res. Toxicol. 23*, 26−36.

(35) Tseng, Y. J., Hopfinger, A. J., and Esposito, E. X. (2012) The great descriptor melting pot: Mixing descriptors for the common good of QSAR models. *J. Comput.-Aided Mol. Des. 26*, 39−43.

(36) Ellman, G. L., Courtney, K. D., Andres, V., Jr., and Featherstone, R. M. (1961) A new and rapid colorimetric determination of acetylcholinesterase activity. *Biochem. Pharmacol. 7*, 88−95.

(37) Ekström, F., Pang, Y.-P., Boman, M., Artursson, E., Akfur, C., and Börjegren, S. (2006) Crystal structures of acetylcholinesterase in complex with HI-6, Ortho-7 and obidoxime: Structural basis for differences in the ability to reactivate tabun conjugates. *Biochem. Pharmacol. 72*, 597−607.

(38) Ekström, F., Hörnberg, A., Artursson, E., Hammarström, L.-G., Schneider, G., and Pang, Y.-P. (2009) Structure of HI-6●Sarin-Acetylcholinesterase Determined by X-Ray Crystallography and Molecular Dynamics Simulation: Reactivator Mechanism and Design. *PLoS One 4*, No. e5957.

(39) Ekström, F., Åstot, C., and Pang, Y.-P. (2007) Novel Nerve-Agent Antidote Design Based on Crystallographic and Mass Spectrometric Analyses of Tabun-Conjugated Acetylcholinesterase in Complex with Antidotes. *Clin. Pharmacol. Ther. 82*, 282−293.

(40) Jakalian, A., Bush, B. L., Jack, D. B., and Bayly, C. I. (2000) Fast, efficient generation of high-quality atomic charges. AM1-BCC model: I. Method. *J. Comput. Chem. 21*, 132−146.

(41) MACCS Keys, MDL Information Systems, Inc., 14600 Catalina Street, San Leandro, CA 94577.

(42) Brown, R. D., and Martin, Y. C. (1996) Use of Structure−Activity Data To Compare Structure-Based Clustering Methods and Descriptors for Use in Compound Selection. *J. Chem. Inf. Comput. Sci. 36*, 572−584.

(43) Sheridan, R. P., Miller, M. D., Underwood, D. J., and Kearsley, S. K. (1996) Chemical Similarity Using Geometric Atom Pair Descriptors. *J. Chem. Inf. Comput. Sci. 36*, 128−136.

(44) Rogers, D. J., and Tanimoto, T. T. (1960) A Computer Program for Classifying Plants. *Science 132*, 1115−1118.

(45) Willett, P., Barnard, J. M., and Downs, G. M. (1998) Chemical similarity searching. *J. Chem. Inf. Comput. Sci. 38*, 983−996.

(46) Dewar, M. J. S., Zoebisch, E. G., Healy, E. F., and Stewart, J. J. P. (1985) Development and use of quantum mechanical molecular models. 76. AM1: a new general purpose quantum mechanical molecular model. *J. Am. Chem. Soc. 107*, 3902−3909.

(47) Labute, P. (2000) A widely applicable set of descriptors. *J. Mol. Graphics Modell. 18*, 464−477.

(48) Labute, P. (2004) Derivation and applications of molecular descriptors based on approximate surface area, in *Chemoinformatics* (Bajorath, J., Ed.), pp 261−278, Humana Press, Totawa, NJ.

(49) Cruciani, G., Crivori, P., Carrupt, P., and Testa, B. (2000) Molecular fields in quantitative structure−permeation relationships: The VolSurf approach. *J. Mol. Struct.: THEOCHEM 503*, 17−30.

(50) Cruciani, G., Pastor, M., and Guba, W. (2000) VolSurf: A new tool for the pharmacokonetic optimization of lead compounds. *Eur. J. Pharm. Sci. 11*, S29−S39.

(51) Cruciani, G., Pastor, M., and Mannhold, R. (2002) Suitability of molecular descriptors for database mining. A comparative analysis. *J. Med. Chem. 45*, 2685−2694.

(52) Stanton, D. T., and Jurs, P. C. (1990) Development and Use of Charged Partial Surface Area Structural Descriptors in Computer-Assisted Quantitative Structure-Property Relationship Studies. *Anal. Chem. 62*, 2323−2329.

(53) Stouch, T. R., and Jurs, P. C. (1986) A simple method for the representation, quantification, and comparison of the volumes and shapes of chemical compounds. *J. Chem. Inf. Comput. Sci. 26*, 4−12.

(54) Hall, L. H., and Kier, L. B. (1991) The Molecular Connectivity Chi Indexes and Kappa Shape Indexes in Structure-Property Modeling, in *Reviews in Computational Chemistry* (Lipkowitz, K. B., and Boyd, D. B., Eds.), pp 367−422, VCH Publishers, Inc., New York.

(55) Hall, L. H., Mohney, B., and Kier, L. B. (1991) The Electrotopological State: An Atom Index for QSAR. *Quant. Struct.-Act. Relat. 10*, 43−51.

(56) Pearlman, R. S., and Smith, K. M. (1998) Novel software tools for chemical diversity. *Perspect. Drug Discovery Des. 9/10/11*, 339−353.

(57) Gasteiger, J., and Marsili, M. (1980) Iterative Partial Equalization of Orbital Electronegativity - A Rapid Access to Atomic Charges. *Tetrahedron 36*, 3219−3228.

(58) Lipinski, C. A., Lombardo, F., Dominy, B. W., and Feeney, P. J. (1997) Experimental and Computational Approaches to Estimate Solubility and Permeability in Drug Discovery and Development Settings. *Adv. Drug Delivery Rev. 23*, 3−25.

(59) Oprea, T. I. (2000) Property Distribution of Drug-Related Chemical Databases. *J. Comput.-Aided Mol. Des. 14*, 251−264.

(60) Lin, A. QuaSAR-Descriptor, Chemical Computing Group, Inc., 1010 Sherbrooke St. W, Suite 910, Montreal, Quebec, Canada H3A 2R7. http://www.chemcomp.com/journal/descr.htm, accessed October 2013.

(61) Wojciechowski, M., and Lesyng, B. (2004) Generalized Born model: Analysis, refinement, and applications to proteins. *J. Phys. Chem. B 108*, 18368−18376.

(62) Devillers, J., Ed. (1996) *Genetic Algorithms in Molecular Modeling*, Academic Press, London.

(63) Holland, J. H. (1975) Adaptation in natural and artificial systems: an introductory analysis with applications to biology, control, and artificial intelligence, University of Michigan, Ann Arbor, MI.

(64) Rogers, D., and Hopfinger, A. J. (1994) Application of genetic function approximation to quantitative structure-activity relationships and quantitative structure-property relationships. *J. Chem. Inf. Comput. Sci. 34*, 854−866.

(65) Shao, J. (1993) Linear model selection by cross-validation. *J. Am. Stat. Assoc. 88*, 486−494.

(66) Opdagelse: Predictive Modeling Toolkit, exeResearch LLC, 32 University Drive, East Lansing, Michigan 48823 USA, http://www.exeResearch.com.

(67) R: A Language and Environment for Statistical Computing, R Development Core Team. R Foundation for Statistical Computing, Vienna, Austria, http://www.R-project.org

(68) Sauer, W. H. B., and Schwarz, M. K. (2003) Molecular shape diversity of combinatorial libraries: a prerequisite for broad bioactivity. *J. Chem. Inf. Comput. Sci. 43*, 987−1003.

(69) Wildman, S. A., and Crippen, G. M. (1999) Prediction of physiochemical parameters by atomic contributions. *J. Chem. Inf. Comput. Sci. 39*, 868−873.